

Hindered and accelerated coalescence of drops in Stokes flow

M. B. Nemer,¹ X. Chen,¹ D. H. Papadopoulos,¹ J. Bławdziewicz,² and M. Loewenberg¹

¹*Department of Chemical Engineering, Yale University, New Haven, Connecticut*

²*Department of Mechanical Engineering, Yale University, New Haven, Connecticut*

(Dated: December 10, 2002)

We analyze axisymmetric near-contact motion of two drops under the action of an external force or imposed flow. It is shown that the far-field stress generated in the near-contact region by the outer flow qualitatively affects drainage of the thin fluid film separating the drops. If this stress acts radially outward, exponential film drainage occurs. For a radially inward far-field stress, film drainage is arrested at long times. An asymptotic analysis of the stationary long-time film profile is developed for small deformation conditions, and the critical strength of van der Waals attraction for film rupture is calculated. Hindered and accelerated drop coalescence have not been predicted by previous theories, because the far-field stress was neglected.

The coalescence of drops brought together by an external force or an imposed flow is largely controlled by the lubrication flow in the thin fluid film between the drop interfaces. Non-hydrodynamic effects (e.g., van der Waals attraction) are significant only during the final stage of film rupture. Thus, the nonlinear evolution of the thin-film region has been the focus of much research [1–9].

The current theoretical descriptions of drop coalescence [4–7] rely on the assumption that under small-deformation conditions the flow field v_∞ produced inside of the drops by their pairwise translational motion or an imposed flow has no effect on film drainage dynamics. Accordingly, no distinction has been made between the film evolution under quiescent or non-quiescent conditions.

This picture is, however, incorrect for drops with tangentially mobile interfaces. As shown in this letter, the flow field v_∞ qualitatively changes film-drainage dynamics for sufficiently thin films (e.g., at long times).

The qualitative effect of an imposed flow on drop coalescence can be understood in terms of the tangential hydrodynamic stress f exerted on the film interfaces by the drop-phase fluid. This stress has two contributions

$$f = f_\infty + f_t. \quad (1)$$

Component f_∞ is associated with the far-field velocity v_∞ , which vanishes at the film interfaces and matches to the externally-driven circulation away from the film. Component f_t is associated with the local flow that is driven by the motion of the film interface and vanishes far from the film.

In previous analyses, the far-field stress component f_∞ was neglected under the assumption that it does not contribute to the balance between the tangential stress and pressure gradient p' in the film,

$$\frac{1}{2}p'h = f, \quad (2)$$

where h is the film-thickness profile.

However, the flow field v_∞ varies on the lengthscale set by the drop size a , and, for drops approaching along

their line of centers, v_∞ vanishes at the symmetry axis. Accordingly, $f_\infty \sim \mu G_0 r_\infty / a$, where μ is the viscosity, G_0 is the magnitude of the far-field velocity gradient, and r_∞ is the radius of the film region. For given external force and imposed flow, p' and r_∞ (thus also f_∞) are nearly independent of h . It follows that $f_\infty \sim hp'$ for sufficiently small h , which implies that the far-field stress component f_∞ must be retained in stress balance (2), in contrast to the current theoretical descriptions.

The boundary-integral simulations and asymptotic analysis presented below confirm the foregoing scaling argument and demonstrate that the far-field stress component can arrest or accelerate film drainage. We consider these effects for axisymmetric near-contact motion of two drops $i = 1, 2$ subjected to body forces and an imposed creeping flow

$$\mathbf{F}_i^e = F_i^e \hat{\mathbf{e}}_z, \quad \mathbf{u}^e = G(\frac{1}{2}r\hat{\mathbf{e}}_r - z\hat{\mathbf{e}}_z). \quad (3a,b)$$

Here (r, z) are cylindrical coordinates with unit vectors $\hat{\mathbf{e}}_r, \hat{\mathbf{e}}_z$ and origin at the center of the gap between the drops; drop (1) is in the halfspace $z < 0$. The suspending fluid has viscosity μ , the drops have viscosity $\lambda\mu$, and the interfacial tension σ is constant. The undeformed-drop radii are a_1, a_2 .

Below, lengths are non-dimensionalized by $a = (a_1^{-1} + a_2^{-1})^{-1}$, stresses by σ/a , force by σa , velocity by σ/μ , and time by $\mu a/\sigma$. In the dimensionless formulation the system dynamics is characterized by the force and flow strength parameters

$$\hat{F}_i^e = \frac{F_i^e}{\sigma a}, \quad \hat{G} = \frac{\mu G a}{\sigma}. \quad (4)$$

Boundary-integral simulations Figures 1 and 2 depict the film evolution for parameter values corresponding, respectively, to a far-field stress directed inward and outward. In the first case, a stationary film profile is attained at long times; in the second case, the film drains exponentially. For $f_\infty = 0$, the film thickness decays algebraically at long times [4, 10, 11]. The current theories

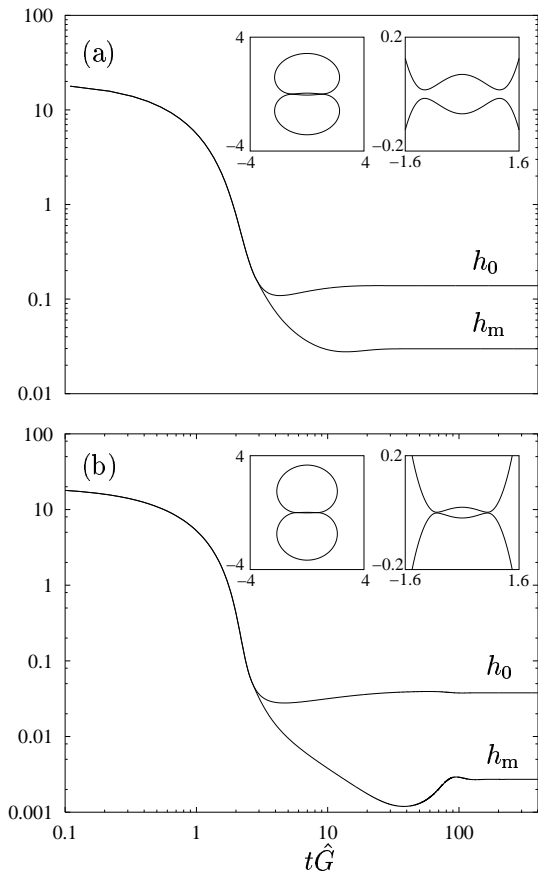


FIG. 1: Evolution of center h_0 and minimum h_m film thickness for equal-size drops with $\lambda = 1$ in straining flow; $\hat{F}_1^e = \hat{F}_2^e = 0$ and (a) $\hat{G} = 0.05$, (b) $\hat{G} = 0.02$. Insets show stationary drop shape and film profile.

neglect the far-field stress component and thus predict algebraic film drainage for all parameter values, in contrast to the numerical results shown above.

Asymptotic analysis For weak forcing $\hat{F}_i^e, \hat{G} \ll 1$, the flow field away from the near-contact region couples to the thin film through (a) hydrodynamic forces F_i^H acting on the drops and (b) the mean of the far-field stresses acting on the film interfaces $f_\infty = \frac{1}{2}(f_\infty^{(1)} + f_\infty^{(2)})$. In the weak-forcing regime, the extent of the thin film region r_∞ is small, and the drops remain nearly spherical; thus, F_i^H and f_∞ correspond to the forces and stresses on spherical drops in point contact.

The hydrodynamic forces on spherical drops are given by a linear resistance relation

$$F_\pm^H = R_{\pm\hat{U}}\hat{U} + R_{\pm\hat{G}}\hat{G}, \quad (5)$$

where $R_{\pm\hat{U}}, R_{\pm\hat{G}}$ are resistance functions (which depend on λ and $k = a_2/a_1$), $F_\pm = F_1 \pm F_2$ are the total and relative forces, and \hat{U} is the dimensionless translational velocity of the drop pair. The total and relative force balances on the drop pair are

$$\hat{F}_+^e + F_+^H = 0, \quad \hat{F}_-^e + F_-^H = 2F_c, \quad (6a,b)$$

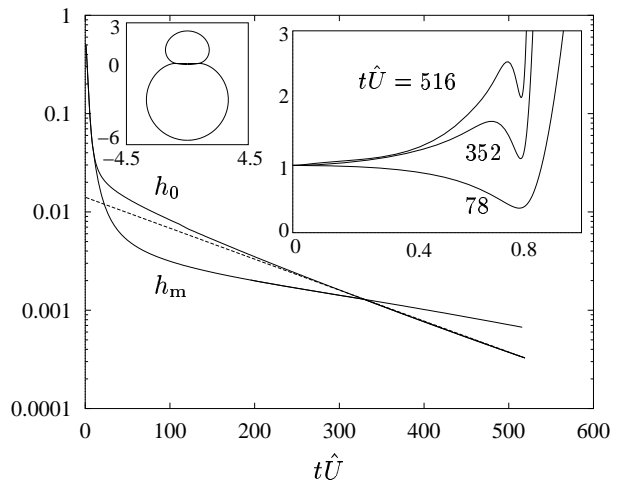


FIG. 2: Evolution of center h_0 and local-minimum h_m film thickness for unequal-size drops with $a_2/a_1 = \frac{1}{2}$ and $\lambda = 1$ in buoyancy motion; $\hat{F}_1^e = 8\hat{F}_2^e = 4\pi$, $\hat{G} = 0$. Exponential fit (dashed line). Insets show long-time drop shape and film profile h/h_0 at indicated times.

where the contact force F_c results from pressure in the deformed near-contact region. The far-field stress component is given by

$$f_\infty = -rS, \quad r\lambda \ll 1, \quad (7)$$

where $f_\infty > 0$ corresponds to an outward-directed stress. By solving the Stokes equations in tangent-sphere coordinates we find

$$\lambda^{-1}S = \frac{(k-1)k}{4(1+k)^3}\hat{U} + \frac{4k-1-k^2}{2(1+k)^2}\hat{G}. \quad (8)$$

The far-field stress f_∞ may be inward or outward directed, resulting in hindered or accelerated film drainage. By Eq. (8), the far-field stress is directed outward for buoyancy-driven motion of unequal size drops $k < 1$, $\hat{U} > 0$ (or $k > 1$, $\hat{U} < 0$) and $\hat{G} = 0$. For drops in axisymmetric compressional flow ($\hat{G} > 0$) with $\hat{F}_+^e = 0$, the far-field stress is directed inward for $k_{\text{crit}}(\lambda) < k < k_{\text{crit}}^{-1}(\lambda)$, and outward for k outside of this range. Equations (8) and (5) (with numerically evaluated resistance functions) yield the critical size ratio $k_{\text{crit}}(\lambda) = 0.351 \pm 0.005$ for $0 < \lambda < \infty$.

Next we consider the stationary thin-film profile $h(r)$ corresponding to an inward-directed far-field stress. The results in Fig. 1 show that the film has a central dome region and a rim region at the edge of the film. The film thickness has a maximum $h_0 = h(0)$ in the dome and a minimum h_m at $r_m \approx r_\infty$ in the rim. For weak forcing, $h \gg h_m$ in the dome, which suggests that the film profile can be obtained by asymptotic matching of the dome and rim regions.

The stationary film profile is calculated using the lubrication approximation [4, 6]. For our problem, the re-

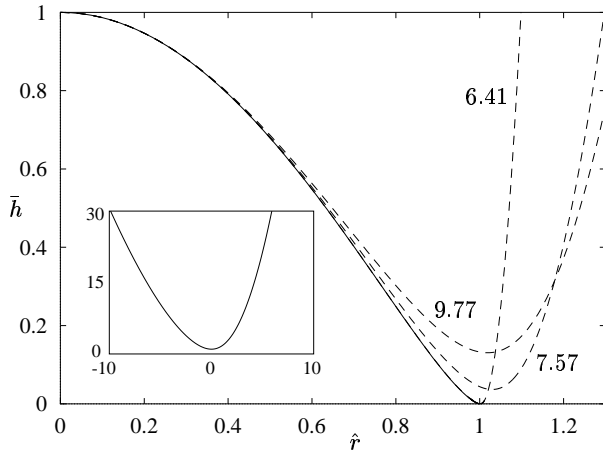


FIG. 3: Solution of dome equations (13) and (15) for indicated values of $B > B^*$ (dashed curves), asymptotic solution $B = B^*$ (solid curve); radial coordinate $\hat{r} = \bar{r}(c/c^*)^{1/2}$, where $c = \bar{h}''(0)$ and $c = c^*$ for $B = B^*$. Inset shows asymptotic solution of rim equations (19) and (21) with $Q = Q^*$.

sulting stress balances in the film are

$$p = 1 - \frac{1}{2}r^{-1}(rh')', \quad hp' = -2rS, \quad (9a,b)$$

where prime denotes differentiation with respect to r . The tangential stress balance (9b) is obtained by inserting relation (7) into (1) and (2). [In Eq. (1) f is the mean of the stresses acting on the film interfaces.] The magnitude of the local stress component is $f_t \sim u_t/l$, where $l \gg h$ is the lateral lengthscale in the film, and u_t is the tangential velocity on the interface. At stationary state, the tangential stress balance gives $u_t \sim f_\infty h$. Accordingly, $f_t \sim (h/l)f_\infty$; thus f_t is neglected in Eq. (9b).

Boundary conditions for the film profile are

$$h'(0) = 0, \quad \lim_{r \rightarrow \infty} p(r) = 0, \quad (10a,b)$$

and the pressure in the film balances the contact force,

$$F_c = 2\pi \int_0^\infty pr dr. \quad (11)$$

Since $p \approx 1$ in the dome and $p \ll 1$ for $r > r_\infty$, the radial location of the rim is approximately

$$r_\infty = (F_c/\pi)^{1/2}. \quad (12)$$

In the dome region, the film equations (9) are rewritten using the variables $\bar{h} = h/h_0$ and $\bar{r} = r/r_m$. Accordingly

$$\bar{h}[\bar{r}^{-1}(\bar{r}\bar{h}')]' = B\bar{r}, \quad (13)$$

where prime denotes differentiation with respect to \bar{r} , and

$$B = 4h_0^{-2}r_m^4 S. \quad (14)$$

The corresponding boundary conditions are

$$\bar{h}(0) = 1, \quad \bar{h}'(0) = 0, \quad \bar{h}'(1) = 0. \quad (15)$$

Numerical solution of boundary-value problem (13) and (15), shown in figure 3, indicates that $\bar{h}_m \rightarrow 0$ for $B \rightarrow B^*$, where

$$B^* = 6.39. \quad (16)$$

Moreover, $\bar{h}''(\bar{r}) \rightarrow \infty$ for $\bar{r} \geq 1$ in this limit. Since $\bar{h}''(\bar{r}) = r_m^2/h_0$ for $\bar{r} \gg 1$ by (9a) and (10b), relation (14) implies that $S \rightarrow 0$ for $B \rightarrow B^*$. Thus the solution $\bar{h}^*(\bar{r}) = \lim_{B \rightarrow B^*} \bar{h}(\bar{r})$ (solid line in Fig. 3) corresponds to the weak-forcing limit $\tilde{F}_i^e, \tilde{G} \ll 1$. In unscaled variables the asymptotic dome shape is

$$h(r) = h_0 \bar{h}^*(\bar{r}), \quad (17)$$

where

$$h_0 = 2(\pi^2 B^*)^{-1/2} F_c S^{1/2}, \quad (18)$$

by Eqs. (12), and (14) (given that $r_m \rightarrow r_\infty$).

To derive the matching solution in the rim region $x = r - r_m \ll r_m$, the film equations (9) are rewritten using variables $\tilde{h} = h/h_m$ and $\tilde{x} = x/h_m^{1/2}$. To leading order in h_m the rescaled film equations are

$$\tilde{h}''' \tilde{h} = Q, \quad (19)$$

where prime denotes differentiation with respect to \tilde{x} and

$$Q = 4h_m^{-1/2} r_m S. \quad (20)$$

The corresponding boundary conditions are

$$\tilde{h}(0) = 1, \quad \tilde{h}'(0) = 0, \quad \lim_{\tilde{x} \rightarrow \infty} \tilde{h}''(\tilde{x}) = 2, \quad (21a,b,c)$$

where the latter follows from Eqs. (9a) and (10b).

Expanding the dome profile $\bar{h}^*(\bar{r})$ around $\bar{r} = 1$ we find

$$\bar{h}^*(1 + \bar{x}) = (\frac{8}{3}B^*)^{1/2}(-\bar{x})^{3/2}, \quad \bar{x} \rightarrow 0^-. \quad (22)$$

Numerical integration of Eqs. (19) and (21) indicates that the rim profile $\tilde{h}^*(\tilde{x})$ with matching asymptotic behavior

$$\tilde{h}^*(\tilde{x}) = (\frac{8}{3}Q)^{1/2}(-\tilde{x})^{3/2}, \quad \tilde{x} \rightarrow -\infty \quad (23)$$

is obtained for $Q = Q^*$, where

$$Q^* = 0.439. \quad (24)$$

The asymptotic solution of the film profile in the rim region $r \approx r_\infty$ for weak forcing is

$$h(r) = h_m \tilde{h}^*(\tilde{x}), \quad (25)$$

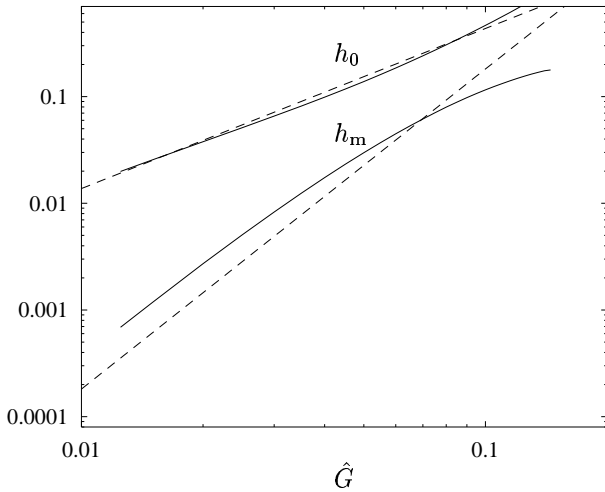


FIG. 4: Stationary center h_0 and minimum h_m film thickness for equal-size drops with $\lambda = 1$ in straining flow versus flow-strength parameter; $\hat{F}_1^e = \hat{F}_2^e = 0$. Numerical simulations (solid lines); asymptotic formulas (18) and (26) (dashed lines).

where $\tilde{h}^*(\tilde{x})$ is shown in Fig. 3. By Eqs. (12) and (20) with $r_m = r_\infty$, the minimum film thickness is

$$h_m = 16(\pi^{1/2}Q^*)^{-2}S^2F_c. \quad (26)$$

In Fig. 4, asymptotic formulas (18) and (26) are compared to boundary-integral simulations for drops in straining flow. Under these conditions, $F_c = \frac{1}{2}R_{-\hat{G}}\hat{G}$, by Eqs. (5) and (6b), which implies that $h_0 \sim \hat{G}^{3/2}$ and $h_m \sim \hat{G}^3$ for $\hat{G} \ll 1$.

For sufficiently thin films, van der Waals attraction is important and can lead to film rupture in the rim. The effect of van der Waals stresses $A(6\pi h^3)^{-1}$ are included by modifying the stationary rim equation (19),

$$\tilde{h}\tilde{h}''' = Q^* - \tilde{A}\tilde{h}'\tilde{h}^{-3}, \quad (27)$$

where A is the Hamaker constant (nondimensionalized by σa^2), and

$$\tilde{A} = 4^{-6}\pi^2(Q^*)^6AS^{-6}F_c^{-3}. \quad (28)$$

Numerical integration of Eq. (27) with boundary conditions (21b,c) and (23) reveals a turning point in the minimal gap at $\tilde{A} = \tilde{A}_{\text{crit}}$, where

$$\tilde{A}_{\text{crit}} = 1.49. \quad (29)$$

For $\tilde{A} < \tilde{A}_{\text{crit}}$ there is a stable and unstable branch of stationary film profiles; there are no stationary solutions for $\tilde{A} > \tilde{A}_{\text{crit}}$.

Accelerated film drainage occurs for an outward-directed far-field stress component $f_\infty > 0$ (corresponding to $S < 0$ in Eq. (7)). For sufficiently thin films,

$p'h \ll f_\infty, f_t$ thus, the appropriate tangential stress balance derived from Eqs. (1) and (2) is

$$f_\infty = -f_t. \quad (30)$$

Given the scalings $f_t \sim u_t/r_\infty$ and $f_\infty \sim r_\infty S$, we find $u_t \sim Sr_\infty^2$. By mass conservation in the film $dh/dt \sim u_t h/r_\infty$ it thus follows that the film drains exponentially at long times

$$dh/dt \sim Sr_\infty h. \quad (31)$$

Figure 2 shows that the above scaling applies in the central region of the film.

We have shown that the tangential stress associated with flow far from the near-contact region hinders film drainage when it acts radially inward, and enhances drainage when it acts radially outward. Thus the effect of this stress must be included in analyses of drop coalescence dynamics. The theory described in this letter can be extended to include Marangoni stresses (surface tension gradients) associated with variations of temperature or chemical and electrical potentials [12–15].

MBN, XC, and ML were supported by NASA grant NAG3-2477, and JB by NASA grant NAG3-2704.

-
- [1] R. K. Jain, I. B. Ivanov, and E. Mardarelli, C. Ruckenstein, in *Dynamics and Instability of Fluid Interfaces*, edited by Sorensen (Springer, Berlin, 1979), p. 140.
 - [2] D. T. Wasan and A. K. Malhotra, *AIChE Symp. Ser.* **82**, 5 (1986).
 - [3] A. K. Chesters, *Trans IChemE* **69**, 259 (1991).
 - [4] S. G. Yiantsios and R. H. Davis, *J. Fluid Mech.* **217**, 547 (1990).
 - [5] S. Hartland, B. Yang, and S. A. K. Jeelani, *Chem. Eng. Sci.* **49**, 1313 (1994).
 - [6] A. Saboni, C. Gourdon, and A. K. Chesters, *J. Colloid Interface Sci.* **175**, 27 (1995).
 - [7] M. A. Rother, A. Z. Zinchenko, and R. H. Davis, *J. Fluid Mech.* **346**, 117 (1997).
 - [8] M. Manga and H. A. Stone, *J. Fluid Mech.* **256**, 647 (1993).
 - [9] H. Yang, C. C. Park, Y. T. Hu, and L. G. Leal, *Phys. Fluids* **13**, 1087 (2001).
 - [10] A. F. Jones and S. D. R. Wilson, *J. Fluid Mech.* **87**, 263 (1978).
 - [11] M. B. Nemer, X. Chen, J. Bławdziewicz, and M. Loewenberg, *Bull. Am. Phys. Soc.* **46**, 140 (2001).
 - [12] P. Dell'Aversana, V. Tontodonato, and L. Carotenuto, *Phys. Fluids* **9**, 2475 (1997).
 - [13] A. Saboni, C. Gourdon, and A. K. Chesters, *Chem. Engng Sci.* **54**, 461 (1999).
 - [14] V. Berejnov, A. M. Leshansky, O. M. Lavrenteva, and A. Nir, *Phys. Fluids* **14**, 1326 (2002).
 - [15] J. S. Eow, M. Ghadiri, A. O. Sharif, and T. J. Williams, *Chem. Eng. J.* **84**, 173 (2001).